DOI: 10.20858/tp.2025.20.3.03

Keywords: gearbox vibrations; drive systems vibrations reduction; damping gear construction

Grzegorz WOJNAR¹, Michał JUZEK²*, Jonas MATIJOŠIUS³, Ádám TÖRÖK⁴

INFLUENCE OF THE GEOMETRICAL PARAMETERS OF SPLIT GEAR ELEMENTS ON THEIR DISPLACEMENT

Summary. Gearboxes are still a key element of drive transmission systems used in various technical objects and many transport means. The gearbox's operation is associated with the emission of vibrations and noise. The quietness of gearboxes is a significant research problem, and in the case of means of transport, it is directly related to the comfort of passengers and the impact on the nearest environment, as it causes pollution with vibrations and noise. The subject of many studies is the search for new and improved design solutions to reduce the vibration emission of operating gearboxes. One such solution is the design of a split gear containing a ring made of a flexible material covered by patent protection, Pat. 244312. This paper assessed the influence of selected geometric parameters of the split gear's flexible ring on the gear elements' displacement due to the transferred load. As part of the research, simulation studies using the finite element method were performed for selected design cases of a split gear and the relative position of the flexible ring and the loaded gear's tooth. The results show a significant effect of the flexible ring's thickness and position relative to the loaded gear's tooth on the displacements of the selected elements.

1. INTRODUCTION

Gearboxes remain a critical element of transmission systems used in many technical objects. They are commonly used in various means of transport and technical objects in the energy sector, and they are used to transfer propulsion in many civil engineering objects. Regardless of their application, the design of gearboxes must meet specific requirements. The obvious ones include ensuring the assumed durability and high reliability [1]. Increasingly often, these requirements also include ensuring the lowest possible emission of vibrations and noise during operation [2-4]. The quiet operation of the gearbox is a key issue in structures that directly affect users and the immediate environment. Such structures undoubtedly include means of transport [5].

In the case of gear transmissions, vibrations generated during their operation have various sources, including parametric vibrations from the shaft's bearings [2, 4, 6-7], deviations resulting from the tolerances of the manufacturing of gearbox elements and their assembly [2, 4, 8], elastic deformations of gearbox elements as a result of transferred loads [1, 2, 4], uneven load distribution along the meshing width [1-4, 9] and housing stiffness [1-4, 10-11]. It should be noted that the main source of vibrations

¹ Silesian University of Technology, Faculty of Transport and Aviation Engineering; Krasińskiego 8, 40-019 Katowice, Poland; e-mail: Grzegorz.Wojnar@polsl.pl; orcid.org/0000-0003-3515-3990

² Silesian University of Technology, Faculty of Transport and Aviation Engineering; Krasińskiego 8, 40-019 Katowice, Poland; e-mail: michal.juzek@polsl.pl; orcid.org/0000-0003-1145-2283

³ Vilnius Gediminas Technical University-VILNIUS TECH, Mechanical Science Institute, Plytinės 25, LT-10105 Vilnius, Lithuania; e-mail: jonas.matijosius@vilniustech.lt; orcid.org/0000-0001-6006-9470

⁴ Budapest University of Tecnology and Economics, Faculty of Transport Engineering and Vehicle Engineering, Department of Transport Technology and Transport Economics; Műegyetem rakpart. 3, 1111 Budapest, Hungary; e-mail: torok.adam@kjk.bme.hu; orcid.org/0000-0001-6727-1540

^{*} Corresponding author. E-mail: michal.juzek@polsl.pl

generated during gearbox operation is the meshing zone, where cooperating gears come into contact. Vibrations from this zone are transferred through the remaining elements of the gearbox (the gear's body, shafts, and bearings) to its housing, thus exciting it. The housing, excited by vibrations in this way, affects the immediate surroundings and the entire object structure in which the gear transmission is installed. In the case of means of transport, this is a highly undesirable phenomenon because vibrations and the noise that accompany them significantly affect passengers and users of transport, reducing their comfort, among other things.

Research to find solutions for reducing the vibration of gearboxes has been conducted for years in many research centers worldwide. Researchers believe it is possible to reduce vibration emissions by, among other methods, using unconventional materials to make gears, which is often supported by additive manufacturing techniques [13-15]. The use of these materials and additive manufacturing techniques is also closely related to the problem of gear manufacturing precision [8, 16-18]. An important direction of research on the development of silent running gearboxes has focused on developing new gear designs and modifying existing ones. In this field, we can distinguish, for example, research aimed at developing new meshing profiles [19-21] and research aimed at developing gears with a modified housing design [14, 22-24].

One of the design solutions for limiting the propagation of vibrations generated in the meshing zone to the other transmission elements is the design of a split gear covered by patent protection, Pat. 244312 [25]. The split gear shown in the patent Pat. 244312 separates the hub and toothed rim by forming a groove in the shape of a sinusoidal curve and then reconnecting these two components with an additional element made of a flexible material called a ring. This design of the gear (Fig. 1) is intended to additionally limit the transfer of vibrations from the meshing zone to the other elements of the gear transmission by using an element (ring) characterized by a higher vibration-damping coefficient than the material from which the hub and the toothed rim are made. Moreover, using an element made of a flexible material is intended to eliminate, to some extent, the negative impact of deviations in the teeth's geometry and reduce uneven load distribution along the tooth width.

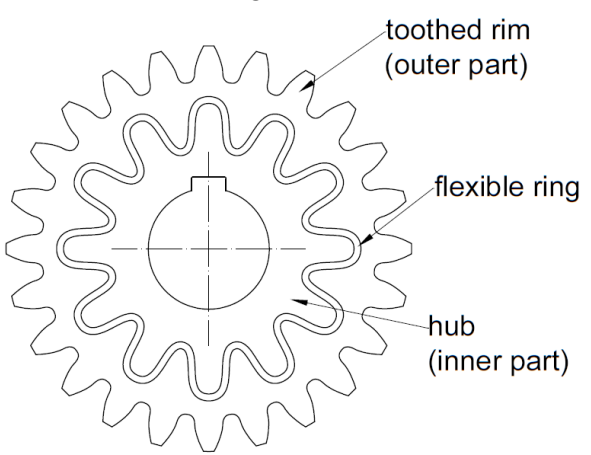


Fig. 1. An illustrative presentation of the split gear design - Pat. 244312

Using a flexible material element in the design of a split gear may contribute to increased displacements of the toothed rim due to the transferred load. Any excessive displacement of the toothed rim could contribute to the deterioration of the meshing conditions of the cooperating teeth, which, in turn, will not bring the expected reduction in vibration emissions from the operating gearbox. This paper assessed the influence of the thickness and shape of the ring, which is made of a flexible element, on the displacements of selected elements of a split gear due to the transferred load. As part of the research, simulation studies using the finite element method (FEM) were performed for selected design cases of a split gear and the relative position of the flexible ring and the loaded gear's tooth. The results reveal

that the flexible ring's thickness and position relative to the loaded gear's tooth significantly affect the displacements of the selected elements.

2. DESCRIPTION OF THE RESEARCH METHOD AND THE CONDUCTED STUDIES

The FEM was used to evaluate the influence of the flexible split ring's selected geometric parameters and its position relative to the loaded gear's tooth on the displacement of selected gear elements. The geometric models of the split gear prepared for simulation consider the geometry changes resulting from the analyzed cases. The selected parameters of the analyzed gear and the transmission in which the gear operated are presented in Table 1.

Table 1 Selected parameters of the gearbox and the analyzed gear

Selected gearbox parameters	
Selected parameter	Value
Gear Ratio - i	1.5
Module - m	4.5 mm
Helix angle - β	0°
Pressure angle - α	20°
Center distance - a_w	91.500 mm
Total unit correction - Σx	0.3532
Circular pitch - p	14.137 mm
Base circular pitch - p_{tb}	13.285 mm
Operating pressure angle - α_w	22.4388°
Selected gear parameters	
Selected parameter	Value
Number of teeth	24
Facewidth - b	20 mm
Unit correction - x_2	0.0497
Pitch diameter - d_2	108.000 mm
Outside diameter - d_{a2}	117.269 mm
Root diameter - d_{f2}	97.198 mm
Base circle diameter - d_{b2}	101.487 mm

In order to accurately represent the load on the gear's tooth during the gearbox operation, an extended analysis was also performed to determine the direction and value of meshing forces for the analyzed gear load cases. Fig. 2 shows the gears' base circles, addendum circles, the line of action (pressure line), and characteristic points. The original drawing was made in the Computer-Aided Design (CAD) environment [26, 27].

Fig. 3 shows an enlarged view of the location of two characteristic points on the line of action. The first of them, marked B1, when the gearbox operates as a reducer, is connected to the end of the single-pair contact and the beginning of the double-pair contact. Similarly, the second of them, marked B2, is connected to the end of the double-pair contact and the beginning of the single-pair contact.

Fig. 4 shows the diameter d_{pB1} related to point B1 (Fig. 3), which marks the end of the single-pair contact and the beginning of the two-pair contact. The diameter of the analyzed gears is d_{pB1} = \emptyset 112.009 mm. The meshing force will be applied to this diameter during further analyses, and its direction is consistent with the direction of the pressure line occurring in the tested gearbox.

Figs. 5a and 5b show two characteristic angles, δ_{pB1} and $\delta_{SB1/2}$. The first of them (δ_{pB1}), which occurs in the case of a gearbox whose axis system O1-O2 is vertical (Fig. 2), is included between the vertical axis Y and the straight line passing through points O2 and B1 (Figs. 3, 5a, and 5b). The second one

 $(\delta_{SB1/2})$, which occurs when the highest tooth of the driven gear is symmetrical to the Y-axis, is included between this axis and the straight line passing through points O2 and $S_{B1/2}$ (Figs. 5a and 5b).

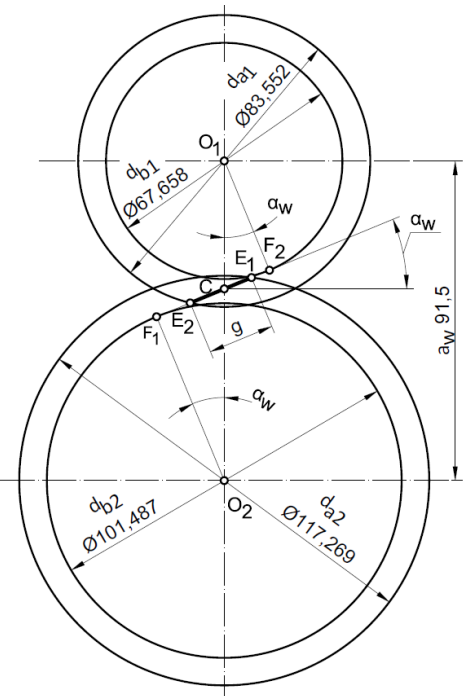


Fig. 2. Base circles and addendum circles of the gears and the line of action (pressure line), as well as characteristic points

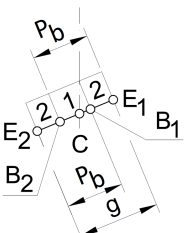


Fig. 3. Characteristic points on the line of action: B1 – end of the single-pair contact and the beginning of the double-pair contact, B2 – end of the double-pair contact and the beginning of the single-pair contact

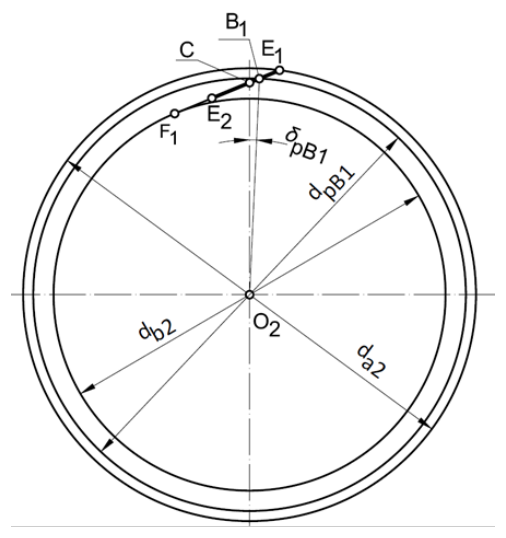


Fig. 4. Driven gear and characteristic diameter d_{pB1} connected with point B1 – end of the single-pair contact and the beginning of the double-pair contact

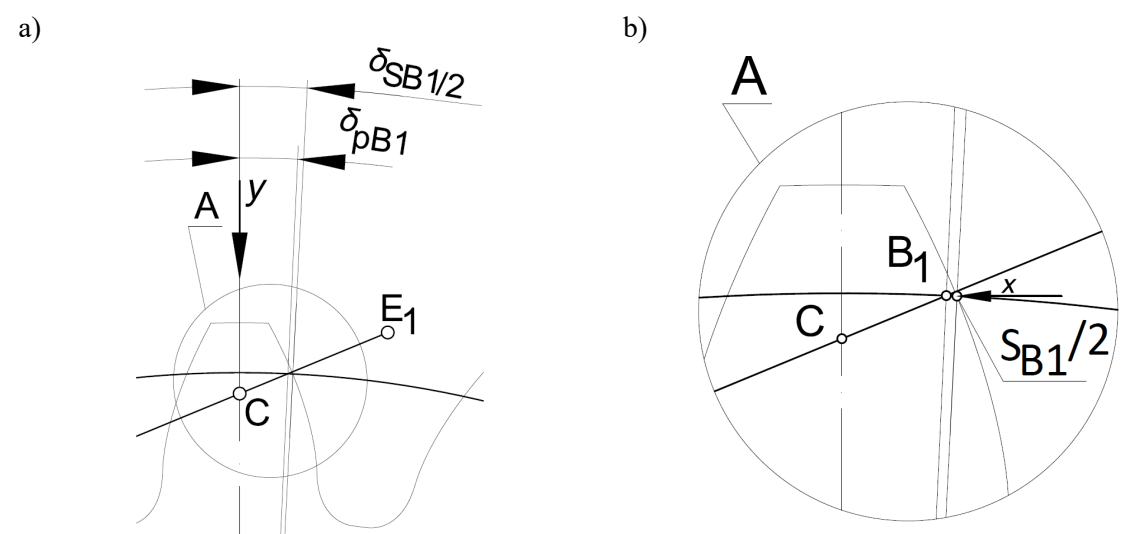


Fig. 5. Two characteristic angles δ_{pB1} and $\delta_{SB1/2}$: a) tooth of the driven gear and two characteristic angles, δ_{pB1} and $\delta_{SB1/2}$, measured concerning the Y-axis – detail A (Fig. 5b) shows the points related to them, and the arms of the angles are led to the point O2; b) the driven gear and the characteristic diameter d_{pB1} related to the end point of the single-pair contact and the beginning of the two-pair contact B1, as well as the point $S_{B1/2}$ located at the intersection of the diameter d_{pB1} and the operating surface of the tooth

Therefore, for further consideration, the gearbox shown in Fig. 2 was adopted, except the axis O1-O2 (Fig. 2) connecting the gears' centers is rotated clockwise relative to point O2 by an angle of $\delta_{SB1/2} - \delta_{pB1}$. In the analyzed case, the value of the angle $\delta_{SB1/2} - \delta_{pB1}$ is 0.2657°. On the other hand, between the horizontal axis X (Fig. 5b) and the direction of the pressure line, there is the angle $\alpha_w - (\delta_{SB1/2} - \delta_{pB1})$. In this case, the highest tooth of the driven gear occupies a symmetrical position to the axis Y (Fig. 5a). The force loading this tooth is applied at the end point of the single-pair contact and the beginning of the two-pair contact B1, which, in this case, coincides with point $S_{B1/2}$ (Fig. 5b). The direction of the meshing force acting along the pressure line determined in this way was reproduced in the model used to conduct the simulation tests (Fig. 6).

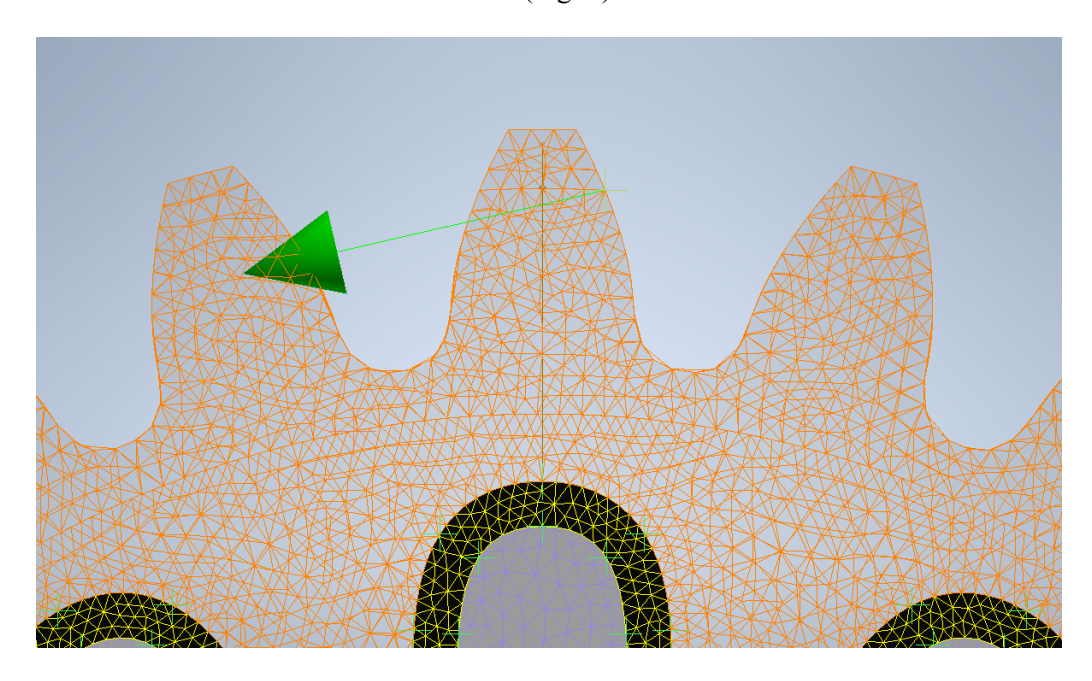


Fig. 6. The direction of the meshing force acting along the pressure line (green vector) reproduced in the model for conducting the simulation tests

The simulation studies aimed to assess the effect of changes in selected geometric parameters of the split gear design on the displacements of the gear components. During these studies, the influence of the thickness of the flexible ring (marked as t_r – Fig. 7) connecting the hub (inner element) and the toothed ring (outer element) of the split gear was analyzed. During the simulation studies, three selected thicknesses of the flexible ring t_r were analyzed: 1 mm, 2 mm, and 3 mm.

The shape of the flexible ring used in the analyzed design of the split gear is characterized by a variable cross-section in the plane containing the axis of rotation of the gear when the value of the angle β_p between the YZ plane and the cross-section plane Π changes (shape similar to a sinusoidal curve).

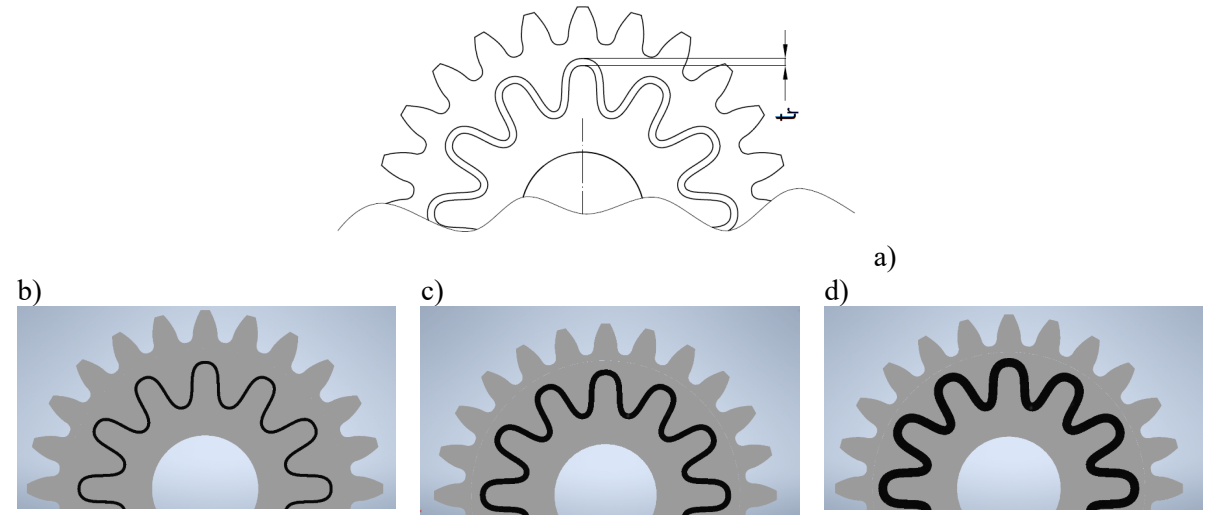


Fig. 7. Graphical representation of the analyzed thicknesses of the flexible ring: a) designation of the thickness of the flexible ring t_r , b) fragment of the gear geometric model used for simulation tests with a flexible ring thickness t_r of 1 mm, c) fragment of the gear geometric model used for simulation tests with a flexible ring thickness t_r of 2 mm, d) fragment of the gear geometric model used for simulation tests with a flexible ring thickness t_r of 3 mm

In addition, the shape of the flexible ring in the circumferential direction is characterized by repeatability, and the angular measure between identical cross-sections of the flexible groove is β_p =30°. Owing to this construction feature of the analyzed split gear, it was also necessary to analyze the influence of changes in the mutual position of the loaded gear tooth (stationary during simulation tests) and the flexible ring on the displacements of the split gear's selected elements. In this study, selected mutual positions of the loaded gear tooth and the flexible ring were analyzed in the range of β_p angles from 0° to 30° in the assumed angular increments of 1.25°. This situation is illustrated in Fig. 8.

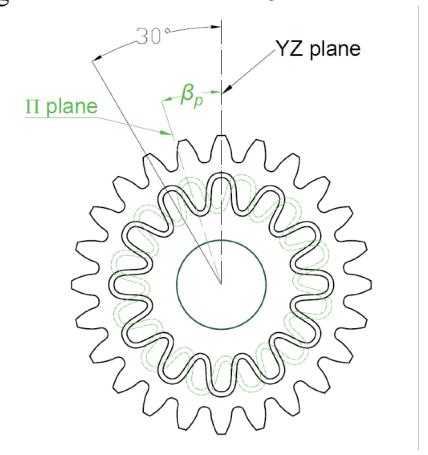


Fig. 8. Illustrative presentation of the angle β_p between the YZ plane and the section plane Π and the analyzed range of angle β_p values from 0° to 30°

Simulation tests were run to analyze four selected cases of the meshing force values representing unit load values Q in the range from 1 MPa to 4 MPa. During the tests, the cylindrical surface of the hub bore was fixed. In the case of gear elements made of metal, the material was AISI 5150 steel. In the case of the flexible ring, the material had linear characteristics reflecting the selected mechanical properties of rubber (i.e., density, Young's modulus, and Poisson's ratio).

3. SIMULATION TEST RESULTS AND THEIR ANALYSIS

In order to determine the displacements of selected elements of the split gear, simulation studies of selected design cases were performed using FEM. Due to the operation of the gear in the real transmission, and in particular the meshing, the same point at the top of the head of the loaded tooth was selected to determine the changes in displacement. The obtained displacement values (relative and absolute) were determined for three significant variants: total displacement, X-axis direction (parallel to the circumferential component of the meshing force axis of action), and Y-axis direction (parallel to the radial component of the meshing force axis of action). Due to the comparative nature of the research, changes in the values of relative displacements between the analyzed cases are presented on a percentage scale (Figs. 9 and 10).

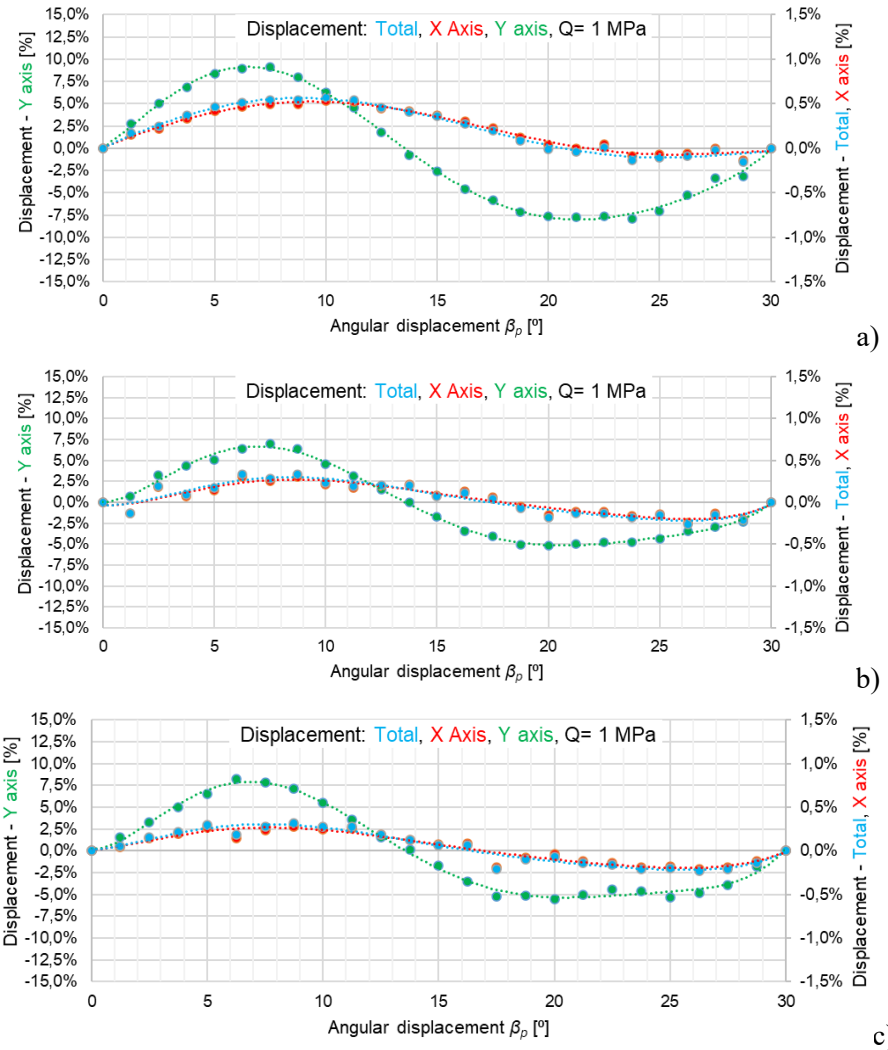


Fig. 9. The course of the obtained displacement values (total, X-axis direction, Y-axis direction) as a function of angular displacement β_p in the case of Q = 1 MPa and a) thickness of the flexible ring $t_r = 1$ mm, b) thickness of the flexible ring $t_r = 2$ mm, c) thickness of the flexible ring $t_r = 3$ mm

In the case of relative total displacements and relative displacements in the circumferential direction (Figs. 9 and 10), the determined courses of their values as a function of the angular displacement β_p are characterized by similar values.

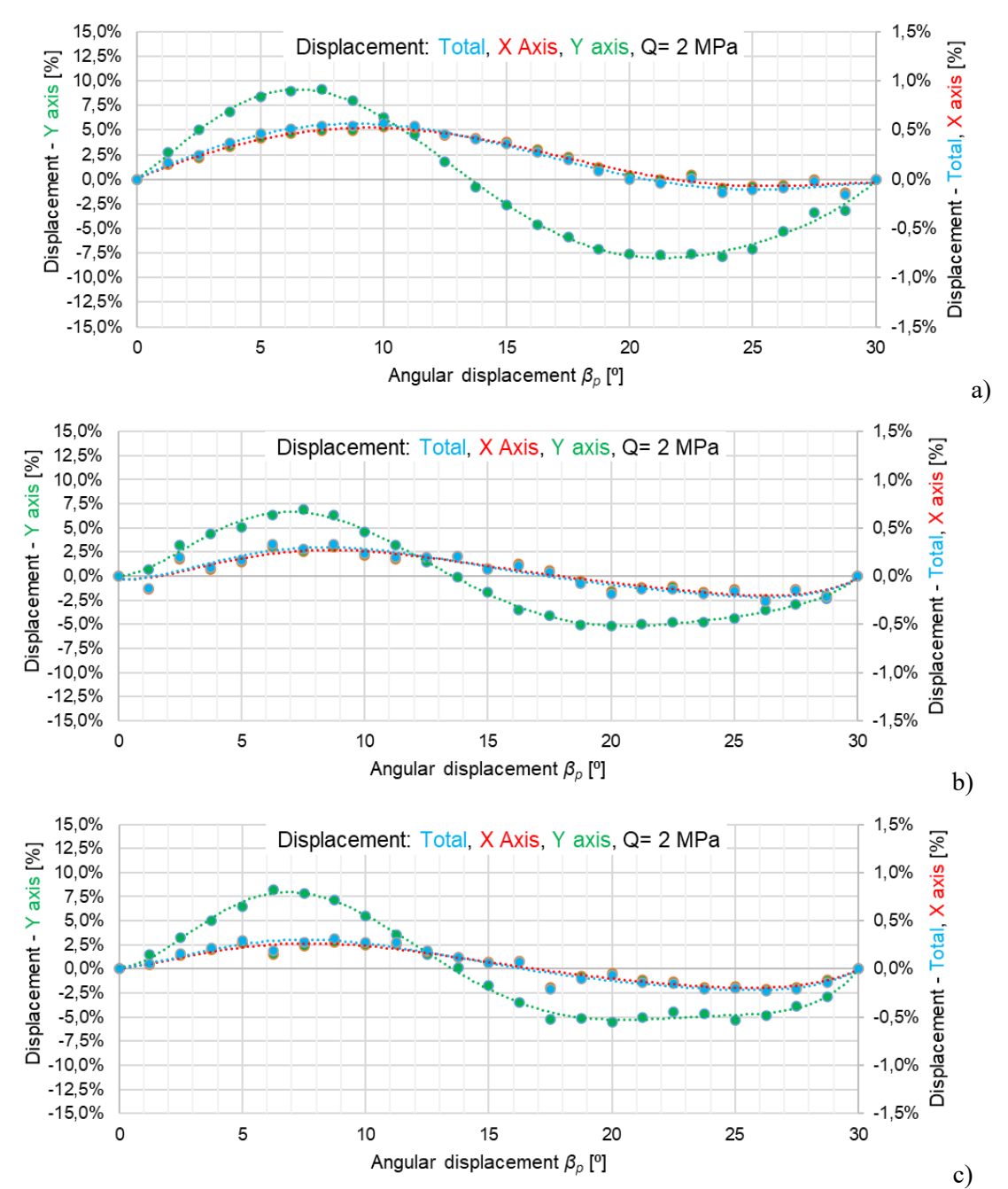


Fig. 10. The course of the obtained displacement values (total, X-axis direction, Y-axis direction) as a function of angular displacement β_P in the case of Q=2 MPa and a) thickness of the flexible ring $t_r=1$ mm, b) thickness of the flexible ring $t_r=2$ mm, c) thickness of the flexible ring $t_r=3$ mm

This is because the displacements in the circumferential direction (the determined actual values of these displacements) in the tested structure of the split gear constitute the dominant component of the calculated total displacement. Moreover, in the case of relative total displacements and relative displacements in the circumferential direction (Figs. 9 and 10), the analysis of the course of the

determined function showed that its zero value occurred in the range of angle β_p values of 16° to 22°, which is not at the point constituting the center of the analyzed range of angular displacement. The highest value of the angular displacement β_p for the zero value point of the determined function was noted for the thickness of the flexible ring $t_r = 1$ mm. As the thickness of the flexible ring increased, the value of the angular displacement β_p for the zero value point decreased. In the case of $t_r = 3$ mm, it was within the range of the angular displacement β_p of 16° to 17°.

The simulation test results show that the largest relative changes in displacements (up to almost 10%) occurred in the Y-axis direction, parallel to the direction of the radial component of the meshing force (Figs. 9 and 10). In this direction, higher displacement values were also observed in the first half of the angular displacement β_p (from 0° to 15°) compared to the second half of the angular displacement β_p (from 15° to 30°). This phenomenon was noted for all analyzed cases. In the case of displacements determined in the Y-axis direction (Figs. 9 and 10), the analysis of the relative displacement change function shows that the zero value point of the determined function occurred in the range of β_p angle values of 13° and 14° , which is also not at the point constituting the center of the analyzed angular displacement range. This phenomenon may result from the direction of the applied meshing force loading the tooth, but an extended analysis is recommended to confirm this thesis.

Fig. 11 presents the displacement curves (actual values) as a function of flexible ring width t_r and selected values of unit load Q for selected cases of angular displacement β_p .

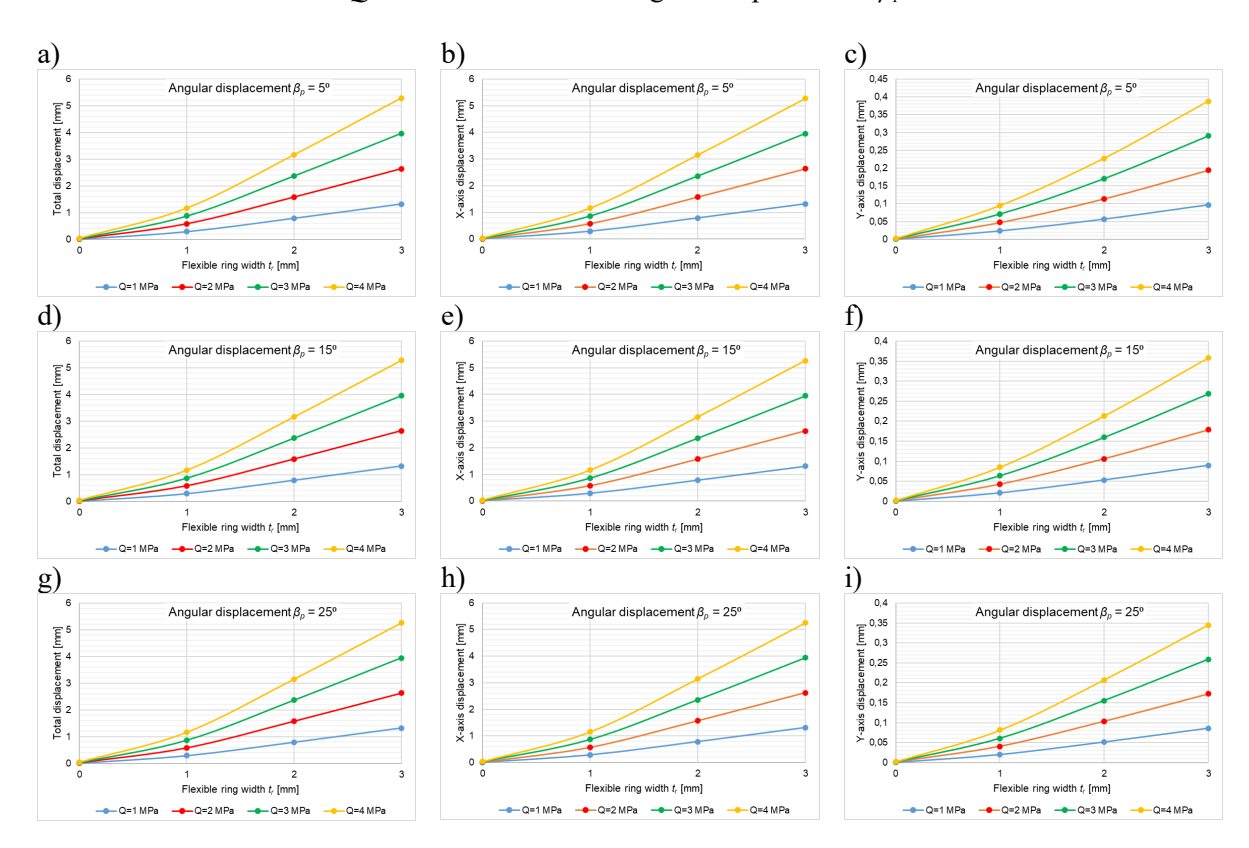


Fig. 11. The course of the obtained displacement values (total, X-axis direction, Y-axis direction) as a function flexible ring width t_r and selected values of unit load Q: a) total displacement and angular displacement $\beta_p = 5^\circ$; b) X-axis direction displacement and angular displacement $\beta_p = 5^\circ$; d) total displacement and angular displacement $\beta_p = 15^\circ$; e) X-axis direction displacement and angular displacement $\beta_p = 15^\circ$; f) Y-axis direction displacement and angular displacement $\beta_p = 15^\circ$; g) total displacement and angular displacement $\beta_p = 25^\circ$; h) X-axis direction displacement and angular displacement $\beta_p = 25^\circ$; h) X-axis direction displacement and angular displacement $\beta_p = 25^\circ$; h) Y-axis direction displacement and angular displacement $\beta_p = 25^\circ$

Based on the courses of the determined displacement functions presented in Fig. 11, the increase in the flexible ring t_r 's thickness results in higher values of total displacements in all analyzed directions. In the case of the values of the flexible ring t_r for the analyzed range of 0 to 3 mm, the course of the determined function is not linear. Moreover, as expected, the increase in the unit load Q also increased the values of total displacements in all analyzed directions.

4. CONCLUSIONS

Based on the simulation tests and analyses of the results, it was found that:

- 1. In the case of a split gear, the selected geometric parameters of the used flexible ring (in particular, the ring thickness) significantly influence the displacement of the split gear's elements due to the transferred load. Based on the courses of the determined displacement functions presented in Fig. 11, it was shown that an increase in the thickness of the flexible ring t_r results in higher values of total displacement in all analyzed directions. In the case of values of thickness of the flexible ring t_r from the analyzed range of 0 to 3 mm, the course of the determined function is not linear.
- 2. In the case of a split gear and the applied shape of the flexible ring (a curve similar to a sinusoid), the position of the loaded gear tooth relative to the flexible ring significantly affects the obtained displacement values of the split gear's elements. The largest relative differences in displacement (almost 10%) were noted for the radial direction (Y-axis direction; Figs. 9 and 10). However, the largest displacements (actual values) were recorded in the circumferential direction (X-axis direction), dominating the calculated value of the total displacement.
- 3. For all analyzed variants and directions of relative displacements, a shift of the zero value point of the determined courses of the above-mentioned displacements relative to the center of the analyzed range of angular displacement ($\beta_p = 15^{\circ}$) was noted. For total displacements and relative displacements in the circumferential direction, the occurrence of the zero value point was demonstrated in the range of the β_p angle values of 16° and 22° (Figs. 9 and 10). The highest value of the angular displacement β_p for the zero point of the determined function was recorded for the thickness of the flexible ring $t_r = 1$ mm. As the thickness of the flexible ring increased, the value of the angular displacement β_p for the zero value point decreased. In the case of $t_r = 3$ mm, it was within the range of the angular displacement β_p of 16° to 17°. In the case of displacements determined in the Y-axis direction (the direction parallel to the direction of the radial component of the meshing force), the analysis of the relative displacement change function showed that the zero value point of the determined function occurred in the range of β_p angle values of 13° and 14° (Figs. 9 and 10). This is also not at the point constituting the center of the analyzed angular displacement range. This phenomenon may result from the direction of the applied meshing force loading the tooth, but an extended analysis is recommended to confirm this thesis.
- 4. In the case of displacements determined in the Y-axis direction (the direction parallel to the direction of the radial component of the meshing force), higher displacement values were observed in the first half of the analyzed range of angular displacement β_p (from 0° to 15°) compared to the second half of the analyzed range of angular displacement β_p (from 15° to 30°; Figs. 9 and 10). This phenomenon was noted for all analyzed cases.

Despite all four of the above important conclusions, this article does not present a detailed analysis of how the proposed design will affect reliability indicators and manufacturing costs. Regarding manufacturing costs, the authors have some experience, having manufactured prototype wheels of this type for research purposes. Manufacturing split wheels costs more than manufacturing non-split wheels because the wheels must be separated and joined with a flexible material. These technological operations had to be developed, which was a significant investment that does not reflect the costs of manufacturing such wheels on a mass scale once the technology has been developed and optimized. However, if experimental studies show that vibrations generated by gears containing split gears are lower, even with higher meshing deviations, the lower cost of producing gears with larger meshing deviations may compensate for the additional steps required to produce split gears.

Furthermore, the authors consider that converting non-split gears, whose teeth exceed acceptable precision classes, into split gears may be cost-effective and ensure lower vibrations during operation. For this reason, the authors plan to conduct this type of research in the future. The authors also plan to conduct reliability tests if positive results are achieved in reducing vibration and noise from transmissions containing split gears. This is because, to limit the number of design variants tested, it is necessary to know which material and its thickness will provide the greatest vibration reduction. This article provides the basis for understanding the phenomena described.

References

- 1. Müller, L. *Przekładnie zębate. Projektowanie*. Warszawa: Wydawnictwo Naukowo-Techniczne. 1996. ISBN: 83-204-1983-2. [In Polish: *Gears. Design*. Warsaw: Scientific and Technical Publishing House].
- 2. Madej, H. *Minimalizacja aktywności wibroakustycznej korpusów przekładni zębatych*. Katowice: Politechnika Śląska. 2003. ISBN: 83-7204-360-4. [In Polish: *Minimization of vibroacoustic activity of gear housings*. Katowice: Silesian University of Technology].
- 3. Łazarz, B. Zidentyfikowany model dynamiczny przekładni zębatej jako podstawa projektowania. Katowice-Radom: Wydawnictwo i Zakład Poligrafii Instytutu Technologii Eksploatacji. 2001. ISBN: 83-7204-249-7. [In Polish: *Identified dynamic model of gear transmission as a basis for design*. Katowice-Radom: Publishing House and Printing Department of the Institute of Exploitation Technology].
- 4. Wilk, A. &, Madej, H. & Łazarz, B. *Wibroaktywność przekladni zębatych*. Katowice-Radom: Wydawnictwo Naukowe Instytutu Technologii Eksploatacji PIB. 2009. ISBN: 978-83-7204-875-2. [In Polish: *Vibration activity of gears*. Katowice-Radom: Scientific Publishing House of the Institute of Exploitation Technology].
- 5. Khan, D. & Burdzik, R. Measurement and analysis of transport noise and vibration: A review of techniques, case studies, and future directions. *Measurement*. 2023. Vol. 220. No. 113354. DOI: 10.1016/j.measurement.2023.113354.
- Krot, P. & Korennoi, V. & Zimroz, R. Vibration-based diagnostics of radial clearances and bolts loosening in the bearing supports of the heavy-duty gearboxes. *Sensors*. 2020. Vol. 20(24). DOI: 10.3390/s20247284.
- 7. Hambric, S.A. & Shepherd, M.R. & Campbell, R.L. & Hanford, A.D. Simulations and measurements of the vibroacoustic effects of replacing rolling element bearings with journal bearings in a simple gearbox. *Journal of Vibration and Acoustics*. 2013. Vol. 135(3). DOI: 10.1115/1.4024087.
- 8. Juzek, M. & Pisula, J. & Žuľová, L. Extended analysis of selected deviations and precision of gears manufacturing as a possibility for reduction of gearboxes' vibroactivity used in means of transport. *Scientific Journal of Silesian University of Technology. Series Transport.* 2025. Vol. 126. P. 65-78. DOI: 10.20858/sjsutst.2025.126.4.
- 9. Wojnar, G. & Juzek, M. The impact of non-parallelism of toothed gear shafts axes and method of gear fixing on gearbox components vibrations. *Acta Mechanica et Automatica*. 2018. Vol. 12(2). P. 165-171. DOI: 10.2478/ama-2018-0026.
- 10. Folega, P. & Burdzik, R. & Wojnar, G. The optimization of the ribbing of gear transmission housing used in transportation machines. *Journal of Vibroengineering*. 2016. Vol. 18. No. 4. P. 2372-2383. DOI: 10.21595/jve.2016.17168.
- 11. Figlus, T. & Kozioł, M. & Kuczyński, Ł. The effect of selected operational factors on the vibroactivity of upper gearbox housings made of composite materials. *Sensors*. 2019. Vol. 19. No. 19. DOI: 10.3390/s19194240.
- 12. Wieczorek, A. & Konieczny, Ł. & Burdzik, R. et al. A complex vibration analysis of a drive system equipped with an innovative prototype of a flexible torsion clutch as an element of preimplementation testing. *Sensors*. 2022. Vol. 22(6). No. 2183. DOI: 10.3390/s22062183.

- 13. Sobczyk, M. & Oleksy, M. & Budzik, G. et al. Polymers in gearbox production. *Polimery*. 2020. Vol. 65. No. 11/12. P. 749-756. DOI: 10.14314/polimery.2020.11.1.
- 14. Scholzen, P. & Billenstein, D. & Hammerl, G. et al. Investigation of the influence of elastic gear body structures on the operational behavior of gears. *Forschung Im Ingenieurwesen/Engineering Research*. 2019. Vol. 83. No. 3. P. 435-444. DOI: 10.1007/s10010-019-00363-4.
- 15. Ramadani, R. & Belsak, A. & Kegl, M. et al. Topology optimization based design of lightweight and low vibration gear bodies. *International Journal of Simulation Modelling*. 2018. Vol. 17. No. 1. P. 92-104. DOI: 10.2507/IJSIMM17(1)419.
- 16. Zajdel, M. & Pisula, J. & Sobolewski, B. et al. Geometrical accuracy of injection-molded composite gears. *Polimery*. 2022. Vol. 67. Nos. 7-8. P. 324-336. DOI: 10.14314/polimery.2022.7.5.
- 17. Pisula, J. The geometric accuracy analysis of polymer spiral bevel gears carried out in a measurement system based on the Industry 4.0 structure. *Polimery*. 2021. Vol. 64. No. 5. P. 353-360. DOI: 10.14314/polimery.2019.5.6.
- 18. Pisula, J. & Budzik, G. & Przeszłowski, Ł. An analysis of the surface geometric structure and geometric accuracy of cylindrical gear teeth manufactured with the direct metal laser sintering (DMLS) method. *Strojniški vestnik Journal of Mechanical Engineering*. 2019. Vol. 65. P. 78-86. DOI: 10.5545/sv-jme.2018.5614.
- 19. Hussein, A.W. & Abdullah, M.Q. High-contact ratio spur gears with conformal contact and reduced sliding. *Results in Engineering*. 2022. Vol. 14. No. 100412. DOI: 10.1016/j.rineng.2022.100412.
- 20. Ye, S.Y. & Tsai, S.J. A computerized method for loaded tooth contact analysis of high-contact-ratio spur gears with or without flank modification considering tip corner contact and shaft misalignment. *Mech Mach Theory*. 2016. Vol. 97. P. 190-214. DOI: 10.1016/j.mechmachtheory.2015.11.008.
- 21. Cheng, Z. & Huang, K. & Xiong, Y. & Han, G. An improved model for dynamic characteristics analysis of high-contact-ratio spur gears considering localised tooth spall defect. *Engineering Failure Analysis*. 2022. Vol. 140. No. 106600. DOI: 10.1016/j.engfailanal.2022.106600.
- 22. Ramadani, R. & Kegl, M. et al. Influence of cellular lattice body structure on gear vibration induced by meshing. *Journal of Mechanical Engineering*. 2018. Vol. 64. No. 10. P. 611-620. DOI: 10.5545/sv-jme.2018.5349.
- 23. Yang, J. & Zhang, Y. & Lee, C.H. Multi-parameter optimization-based design of lightweight vibration-reduction gear bodies. *Journal of Mechanical Science and Technology*. 2022. Vol. 36. No. 4. P. 1879-1887. DOI: 10.1007/s12206-022-0325-1.
- 24. Medvecká-Beňová, S. Analysis of gear wheel body influence on gearing stiffness. *Acta Mechanica Slovaca*. 2017. Vol. 21. No. 3. P. 34-39. DOI: 10.21496/ams.2017.024.
- 25. Patent 244312. *Gear wheel to reduce the transmission of vibrations*. Silesian University of Technology, Gliwice. 19.10.2023.
- 26. Alzyod, H. & Ficzere, P. Finite element modeling of additive manufacturing in case of metal parts. *Periodica Polytechnica Transportation Engineering*. 2022. Vol. 50. No. 4. P. 330-335. DOI: 10.3311/PPtr.19242.
- 27. Aljawabrah, A. Analysis and Control of the Gearshift Process Based on a Dog Clutch Shiftability Model. *Cognitive Sustainability*. 2024. Vol. 3(3). P. 50-70. DOI: 10.55343/cogsust.120.

Received 29.06.2024; accepted in revised form 18.08.2025